Highly polarized structures in the near-nuclear regions of Cygnus A: intrinsic anisotropy within the cones?

C.N. Tadhunter[1], **W. Sparks**[2], **D.J. Axon**[3], **L. Bergeron**[2], **N.J. Jackson**[4], **C. Packham**[5], **J.H. Hough**[3], **A. Robinson**[3], **S. Young**[3]

[1]Department of Physics, University of Sheffield, Sheffield S3 7RH, UK
[2]Space Telescope Science Institute, 3700 San Martin Drive, Baltimore, MD 21218, USA
[3]Division of Physics and Astronomy, Department of Physical Sciences, University of Hertfordshire, College Lane, Hatfield, Herts AL10 9AB, UK
[4]Nuffield Radio Astronomy Laboratory, Jodrell Bank, University of Manchester, UK
[5]Isaac Newton Group, Sea Level Office, Apartado de Correos, 321, 38780 Santa Cruz de La Palma, Islas Canarias, Spain

Abstract. We present near-IR imaging polarimetry observations of the nucleus of Cygnus A, taken with the NICMOS camera of the HST at a wavelength of 2.0μm. These maps reveal a highly collimated region of polarized emission straddling the nucleus and extending to a radius of 1.2 arcseconds. Remarkably, this feature coincides with one, but only one, limb of the edge-brightened bicone structure seen in the total intensity image. The high degree ($P_k \sim 25\%$) and orientation of the extended polarization feature are consistent with a scattering origin. Most plausibly, the detection of polarization along only one limb of the bicone is a consequence of *intrinsic anisotropy* of the near-IR continuum within the radiation cones, with the direction of maximum intensity of the near-IR radiation field significantly displaced from the direction of the radio axis. The unresolved nuclear core source is also highly polarized ($P_k > 28\%$), with a position angle close to the perpendicular to the radio axis. Given that this high degree of nuclear polarization can only be explained in terms of dichroic extinction if the dichroic mechanism is unusually efficient in Cygnus A, it is more likely that the nuclear polarization is due to the scattering of nuclear light in an unresolved scattering region close to the AGN. In this case, the flux of the core source in the K-band is dominated by scattered rather than transmitted quasar light, and previous extinction estimates based on K-band photometry of the core substantially underestimate the true nuclear extinction.

1 Introduction

As yet, little is known about the structure of the inner regions of powerful radio galaxies and the impact of the activity on circumnuclear regions. The high resolution and sensitivity afforded by imaging observations using the Hubble Space Telescope (HST) has revealed a wealth of complex structures in such objects, with dust lanes, jets and large regions of scattered emission from hidden nuclei. One of the key targets in studies which aim to elucidate the interplay between active nuclei and their host galaxies, and between galactic activity of different types, is the archetypal powerful radio galaxy Cygnus A (see Carilli & Barthel 1996 for a review).

HST infrared imaging observations of Cygnus A by Tadhunter *et al.* (1999) revealed an edge-brightened bi-conical structure centred on the nuclear point source, which is strikingly similar to those observed around young stellar objects. The edge-brightening of this structure provides evidence that the bicone is defined as much by outflows in the nuclear regions as by the polar diagram of the illuminating quasar radiation field. The HST observations also show an unresolved nuclear source at 2.0 and 2.25μm. However, from the imaging observations alone it is unclear whether this unresolved source represents the highly extinguished quasar nucleus seen directly through the obscuring torus, or emission from a less-highly-extinguished extended region around the nucleus.

Near-IR polarization observations have the potential to remove the uncertainties surrounding the nature of the unresolved nuclear sources and, in addition, to provide further important information about the obscuration and anisotropy in the near-nuclear regions of powerful radio galaxies. Previous ground-based polarimetric observations of Cygnus A by Packham *et al.* (1998) demonstrate that the nuclear regions are highly polarized in the K-band, with a measured polarization of $P_k \sim 4\%$ for a 1 arcsecond diameter aperture centred on the compact IR nucleus. However, the resolution of the ground-based observations is insufficient to resolve the structures and determine the polarization mechanism unambiguously. In this letter we present new diffraction-limited infrared imaging polarimetry observations of Cygnus A made with the Near Infrared Imaging Camera and Multi-Object Spectrometer (NICMOS: MacKenty *et al.* 1997) on the HST. These observations resolve the polarized structures, and raise new questions about the nature of the anisotropy in the near-nuclear regions of this key source.

2 Observations and data reduction

NICMOS Camera 2 'long wavelength' infrared imaging polarization observations were taken December 1997 and August 1998, giving a pixel scale of 0.075 arcseconds and a total field of 19.4×19.4 arcseconds. The NICMOS polarizers are self-contained spectral elements, with the three long wavelength polarizers effective from $\lambda \approx 1.9$—2.1μm, resulting in an effective central wavelength of $\approx 2.0\mu$m (MacKenty *et al.* 1997). The polarizers are oriented at approximately 60° intervals and have characteristics as presented by Hines (1998). Each exposure consisted of a number of non-destructive reads of the detector which were optimally combined in the reduction software to remove cosmic rays. Regular chops were made to offset fields in order to facilitate accurate background subtraction. The total integration time was 2400 seconds per polarizer.

The reduction of the data used standard IRAF/STSDAS pipeline processing together with pedestal removal as given by van de Marel (1998). The three final, clean polarization images were combined following the prescription of Sparks & Axon (1999), using the pipeline produced variance data. The output data comprised a set of images containing each of the Stokes parameters I, Q, U, their variances and covariances, a de-biassed estimate of the polarization intensity and polarization degree using the method of Serkowski (1958), and also position angle and uncertainty estimates on each of those images, as described in detail in Sparks & Axon (1999).

The two epochs of observation were acquired with different instrumental orientation,

and were analysed independently to provide a robust check on our estimated uncertainties and on the possibility of systematic errors. A variety of spatial resolutions were used, from full diffraction-limited NICMOS resolution down to ≈ 1 arcsec by smoothing the input three images prior to polarization analysis. Both epochs were fully consistent within the estimated statistical errors, implying that there are no significant sources of systematic uncertainty. Measurements of several Galactic stars in the field of Cygnus A give $2.0\mu m$ polarizations of $P_{2.0\mu m} < 2.0\%$ for 5 pixel diameter apertures. This can be regarded as an upper limit on the level of systematic error in estimates of P. The typical statistical uncertainties for the most highly polarized regions measured in our full resolution images are $\pm 1.5\%$ for P, and $\pm 3°$ for the polarization angle. In the following, we will present the data for the December 1997 observations only, since these have a higher S/N as a consequence of longer exposure times.

3 Results

Figure 1 shows the first epoch polarization results. As expected, the total intensity image (Stokes I) is very similar to the direct images published previously by Tadhunter et $al.$ (1999). In particular, it shows an apparent edge-brightened, reasonably symmetric, bi-conical structure centred on the nucleus with an opening angle of 116 degrees and whose axis is closely aligned with the large scale radio jet.

The image of polarized intensity, however, reveals intriguing differences compared to total intensity. The only regions of strongly polarized emission (apart from the nucleus discussed below) are confined to a quasi-linear structure running along the NW-SE limb of the bi-conical structure. This feature shows approximate reflection symmetry about the nucleus, as opposed to the axial symmetry about the radio axis in the total intensity image. The brightness ratio of the two limbs of the cone to the east of the nucleus is approximately 2:1 in total intensity image, while in polarized intensity image it is >12:1. Note that the polarization structure visible in our $2.0\mu m$ image is strikingly different from that of the optical V- and B-band polarization images (Tadhunter et $al.$ 1990, Ogle et $al.$ 1997), in which the polarized emission appears uniformly distributed across the kpc-scale ionization cones and shows no clear preference for the NW-SE limb of the bi-cone.

Typical $measured$ degrees of polarization are in excess of 10% up to a maximum of $\approx 25\%$ in the polarized region to the south east of the nucleus. However, these measures underestimate the true degree of $intrinsic$ polarization in the extended structures, because starlight from the host galaxy makes a substantial contribution to the total flux. For example, using the azimuthal intensity profile measured in annulus with inner radius 4 pixels and outer radius 12 pixels, we estimate that the diffuse starlight from the host galaxy contributes 50 - 70% of the total flux in the south east arm of the bicone. Assuming that the starlight is unpolarized, the degree of intrinsic polarization in the south east arm is $P_{2.0\mu m}^{intr} \sim 50 - 70\%$. Such high degrees of measured and intrinsic IR polarization are unprecedented in observations of active galaxies in which the synchrotron emitting jets are not observed directly at infrared wavelengths.

3.1 The nucleus

The nuclear point source, discussed in detail by Tadhunter *et al.* (1999), is also highly polarized. In the polarized intensity image the main nuclear component appears unresolved ($FWHM = 2.24$ pixels) and its position agrees with that of the nucleus in the total intensity image to within 0.5 pixels (0.04 arcseconds). Thus, it appears likely that the bulk of the polarization is associated with the compact nucleus rather than a more extended region around the nucleus. The core does, however, show a faint entension to the NW in the polarized intensity image. This extension is aligned with the larger scale polarization structures, and its polarization E-vector is close to perpendicular to the radius vector from the nucleus.

From our full resolution polarization images, the measured degree of polarization at the peak flux of the nuclear point source is $P^m_{2.0\mu m} \sim 20\%$. However, spurious polarization can arise because of small mis-alignments between the polarization images, especially in the nuclear regions where there are sharp gradients in the light distribution. To guard against such effects we have smoothed the polarization data using a 5×5 pixel boxcar filter (0.375×0.375 arcseconds) and re-measured the polarization in the nuclear regions. As expected, the measured degree of polarization in the nucleus in the smoothed image is less ($P^m_{2.0\mu m} \sim 10\%$) than in the full resolution image, because of the greater degree of contamination by unpolarized starlight and extended structures around the nucleus. In order to determine the intrinsic polarization of the point source it is necessary to first determine the proportion of flux contributed by the point source to the total flux in the nuclear regions. Experiments involving the subtraction of a Tiny Tim generated point spread function (Krist & Hook 1997) suggest that an upper limit on the fractional contribution of the nucleus to the total flux in a 5×5 pixel pixel box centred on the nucleus is $f_{nuc} < 35\%$. Thus, assuming that *all* the polarization in the near-nuclear regions is due to the unresolved compact core, and that the remainder of the light is unpolarized, the intrinsic polarization of the unresolved core source is $P^{intr}_{2.0\mu m} = P^m_{2.0\mu m}/f_{nuc} > 28\%$.

The position angle of polarization E-vector of the core source measured in our full resolution polarization map ($PA = 201 \pm 3$), is close to perpendicular to the radio jet axis ($PA = 105 \pm 5$). This is similar to the situation seen in other AGN, and in particular Cen A, where, towards longer wavelengths and smaller apertures, the infrared polarization becomes more and more closely perpendicular to the radio jet (Bailey *et al.* 1986).

4 Discussion

4.1 The nature of the unresolved core source

A major motivation for the HST observations was to investigate the nature of the compact core source and the cause of the relatively large polarization measured in the core by Packham *et al.* (1998). The explanation favoured by Packham *et al.* is that the compact core source represents transmitted quasar light, while the high polarization is due to dichroic absorption by aligned dust grains in the central obscuring torus. Because the dichroic mechanism is relatively inefficient, a high polarization implies a large extinction: from observations of Galactic stars it is known that *at least* 55 magnitudes of visual ex-

tinction is required to produce a K-band polarization of 28% for optimum grain alignment (Jones 1989). More typically, the correlation between K-band polarization and extinction deduced for Galactic stars by Jones (1989) implies that an extinction of $A_v \sim 350$ magnitudes would be required for $P_k = 28\%$. For comparison, an upper limit on the K-band extinction in Cygnus A, estimated by comparing the 2.25μm core flux with mid-IR and X-ray fluxes, is $A_v < 94$ magnitudes (see Tadhunter *et al.* 1999 for details). Thus, the dichroic mechanism is only feasible if the efficiency of the mechanism in Cygnus A is greater than it is along most lines of sight in our Galaxy. Such enhanced efficiency cannot be entirely ruled out, given that the Galactic dichroic polarization involves a randomly oriented magnetic field component, whereas the magnetic fields in the central obscuring regions of AGN may be more coherent. In this context it is notable that near- and mid-IR polarization measurements of the central regions of the nearby Seyfert galaxy NGC1068 provide evidence for a greater dichroic efficiency than predicted by the Jones (1989) correlation, with $P_k = 5\%$ produced by $A_v \sim 20 - 40$ magnitudes (Lumsden et al. 1999). However, even the greater dichroic efficiency deduced for NGC1068 would not be sufficient to produce the high polarization measured in the core of Cygnus A if $A_v < 94$ magnitudes.

The efficiency problem might be resolved if the extinction to the core source in the K-band is higher than the $A_v < 94$ estimated on the basis of comparisons of the K-band flux with the mid-IR and X-ray fluxes. Indeed, substantially higher extinctions have been deduced for Cygnus A, both from modelling the X-ray spectrum of the core ($A_v = 170\pm30$: Ueno *et al.* 1994) and from comparisons between hard-X-ray continuum, [OIII] emission line and mid-infrared continuum fluxes ($A_v = 143\pm35$: Ward 1996, Simpson 1995). If such high extinctions also apply to the quasar nucleus in the K-band, the low efficiency of the dichroic mechanism would be less of a problem. However, for any reasonable quasar SED, the contribution of such a highly obscured quasar nucleus to the flux and the polarization of the *detected* 2.0μm core source would be negligible (i.e. we would not expect to detect the quasar nucleus directly in the K-band). Thus, it is more likely that the relatively low extinction deduced from the K-band flux measurements reflects contamination of the K-band core by emission from a less-highly-obscured region, which is close enough to the central AGN to remain unresolved at the resolution of our HST observations. Although it has been proposed that the contaminating radiation in the K-band may include hot dust emission and/or line emission from quasar-illuminated regions close to the nucleus (e.g. Stockton & Ridgway 1996), such emission would have a low intrinsic polarization, and a large dichroic efficiency would still be required in order to produce the polarization of this component by dichroism.

The most plausible alternative to dichroic extinction is that the K-band core source represents scattered- rather than transmitted quasar light. In this case, the polarization is a consequence of scattering in an unresolved region close to the illuminating quasar; we do not detect the quasar nucleus directly in the K-band; and previous extinction estimates based on the K-band fluxes substantially underestimate the true nuclear extinction. Note that the presence of such a scattered component would resolve the discrepancy between the extinction estimates based on K-band flux measurements, and those based on fluxes measured at other wavelengths.

Finally, we must also consider the possibility that the core polarization is due to synchrotron radiation associated with the pc-scale jet visible in VLBI radio images (Krich-

baum *et al.* 1996). Although the *integrated* polarization of the radio core is small even at high radio frequencies ($P_{22GHz} < 5\%$: Dreher 1979), we cannot entirely rule out the possibility that we are observing a highly polarized sub-component of the jet which suffers a relatively low extinction, or alternatively that the radio core source as a whole suffers large Faraday depolarization at radio wavelengths, and would appear more highly polarized at infrared wavelengths. Polarization observations at sub-mm wavelengths will be required to investigate this latter possibility.

4.2   The extended polarization structures

An intriguing feature of our HST observations is the high degree of polarization measured along, and only along, the NW-SE limb of the bicone. The orientation of the polarization measured along the limb is consistent with the scattering of light from a compact illuminating source in the nucleus, while the high degree of polarization is consistent with the edge-brightened bi-cone geometry of Tadhunter *et al.* (1999), in the sense that the scattering angle for the edge-brightened region will be close to the optimal 90° required for maximal polarization. However, the fact that the polarization is measured along only one limb is difficult to reconcile with the simplest bicone model in which the illuminating IR radiation field is azimuthally isotropic, and the scattering medium is uniformly distributed around the walls of the funnels hollowed out by the circum-nuclear outflows. In this simplest model both limbs would be highly polarized in the direction perpendicular to the radius vector of the source, and this is clearly inconsistent with the observations.

Our observation require that one or more of the assumptions implicit in the simple model must be relaxed. In general terms this requires either invoking specific matter distributions within the cone and/or an anisotropic illumination pattern of the central source itself.

Perhaps the simplest way of reconciling the polarization characteristics with the bi-cone geometry is to adjust the relative importance of scattering and intrinsic emmission with azimuth around the cone, so that one limb of the cone is dominated by scattered radiation, while the other is predominatly intrinsic radiation. Since the band-pass of the NICMOS polarizers contains the Paschen alpha line, this provides an obvious potential source of the diluting radiation for the unpolarized regions. Unfortunately there is no obvious reason why such an asymmetry should exist. Furthermore, direct images with the F222M filter show that there is no radical change in the relative brightness of the two limbs of the eastern cone between 2.0μm and 2.25μm. This is an argument against the Paschen alpha model for the intrinsic emission, since the F222M filter admits no emission lines as strong as Paschen alpha.

An alternative possibility is that the NW-SE limb is brighter because the near-IR radiation field of the illuminating AGN is more intense in that direction (i.e. the illuminating radiation field is azimuthally anisotropic within the cones). In this case, the clear difference in structure between the optical and near-IR reflection nebulae suggests that the sources of illumination at the two wavelengths are different: while the source of the shorter wavelength continuum must produce a radiation field which is azimuthally isotropic within cones defined by the obscuring torus, the source of illumination at the longer wavelengths is required to display considerable degree of azimuthal anisotropy.

The near-IR continuum source must also have a relatively red spectrum, in order to avoid producing similar structures at optical and infrared wavelengths. The near-IR anisotropy might arise in the following ways.

1. **Beamed radiation from the inner radio jet.** The near-IR continuum is emitted by a component of the inner synchrotron jet which has a direction of bulk relativistic motion siginificantly displaced from the axis of the large-scale radio jet, such that the radiation is beamed towards the NW-SE limb of the bicone. However, given the remarkable degree of collimation, and the lack of bending, observed in the Cygnus A jet on scales betweem 1pc and 100kpc, a major difficulty with this model is that the the jet would have to bend through a large angle on a scale smaller than ∼1pc (the resolution of the VLBI maps), whilst retaining the rotational symmetry in the jet structure about the nucleus. A further requirement of this model is that, if the inner jet is precessing, the precession timescale must be greater than the light travel time (∼5000 years) across the bicone structure.

2. **Anisotropic hot dust emission.** The near-IR continuum is emitted by hot dust in the inner regions of the galaxy, with a larger projected area of the emitting region visible from one limb of the bicone than from the other. For example, if the near-IR radiation is emitted by dust in a warped disk close to the central AGN — perhaps an outer part of the accretion disk — the warp could be oriented such that the NW-SE limb has an almost face-on view of the emitting region, whereas the the NE-SW limb has a more oblique view. There is already direct observational evidence for a warped outer accretion disk in at least one active galaxy (Miyoshi *et al.* 1995). Given that this mechanism would produce a relatively mild, broad-beam anisotropy, an optically thick torus on scales larger than the hot dust emitting region would still be required in order to produce the sharp-edges to the illuminated bicone structure.

Note that regardless of how any anisotropy in the IR radiation field might be produced, such anisotropy would not by itself explain the nature of the unpolarized emission along the SW-NE limb of the bicone, and the lack of variation in the brightness ratio of the two limbs of the eastern cone between 2.0μm and 2.25μm. It may also be difficult to reconcile the anisotropic illumination model with the polarization properties of the unresolved core source: if the core polarization is due to scattering, the orientation of the core polarization vector implies that a substantial flux of illuminating photons must escape at large angles to the NW-SE limb of the bicone.

We expect future spectropolarimetry observations to resolve the uncertainties concerning the origin of the near-IR polarization structures in Cygnus A. For example, in the case of the anisotropic illumination mechanisms considered above, the anisotropy is in the *continuum* flux rather than the broad lines associated with the AGN. Thus, if this model is correct, the broad lines will be relatively weak or absent in the polarized spectrum of the extended structures. In contrast, for a non-uniform distribution of scattering material but isotropic illumination within the cones, the broad lines and continuum will be scattered equally, and the equivalent widths of the broad lines in the polarized spectrum should fall within the the range measured for steep spectrum radio quasars.

5 Conclusions and Future Work

Our NICMOS polarimetry observations of Cygnus A have demonstrated the existence of a compact reflection nebula around the hidden core, but one whose polarization properties are inconsistent with the simplest illumination model suggested by the imaging data. The predominantly axial symmetry of the total intensity imaging is replaced by axial asymmetry and reflection symmetry about the nucleus in polarized light.

We have discussed several mechanisms to explain the near-IR polarization structures. While none of these is entirely satisfactory, it is clear that the near-IR polarization properties have the potential to provide key information about the geometries of the central emitting regions in AGN, and the near-IR continuum emission mechanism(s). In this context, it will be interesting in future to make similar observations of a large sample of powerful radio galaxies in order to determine whether the extraordinary IR polarization properties of Cygnus A are a common feature of the general population of such objects.

References

Bailey, J.A., Sparks, W.B., Hough, J.H., Axon, D.J., 1986, Nat, 332, 150

Carilli C., Barthel, P.D., 1996, A&ARev, 7, 1

Dreher, J.W., 1979, ApJ, 230, 687

Hines, D.C., 1998, NICMOS & VLT, ESO Workshop and Conference Proceedings, 55, Wolfram Freudling and Richard Hook (eds), p63

Jones, T.J., 1989, ApJ, 346, 728

Krichbaum, T.P., Alef, W., Witzel, A., 1996, in Cygnus A — Study of a Radio Galaxy, ed. C.L. Carilli & D.E., Harris (Cambridge: Cambridge University Press), 93.

Krist J.E., Hook, R., 1997, TinyTim User Guide, Version 4.4 (Baltimore:STScI)

Lumsden, S.L., Moore, T.J.T., Smith, C., Fujiyoshi, T., Bland-Hawthorn, J., Ward, M.J., 1999, MNRAS, 303, 209

MacKenty J.W., *et al.* 1997, NICMOS Instrument Handbook, Version 2.0 (Baltimore: STScI)

Miyoshi, M., Moran, J., Herrnstein, J., Greenhill, L., Nakai, N., Diamond, P., Inoue, M., 1995, Nature, 373, 127

Ogle P.M., Cohen, M.H., Miller, J.S., Tran, H.D., Fosbury, R.A.E., Goodrich, R.W., 1997, ApJ, 482, L37

Packham, C., Hough, J.H., Young, S., Chrysostomou, A., Bailey, J.A., Axon, D.J., Ward, M.J., 1996, MNRAS, 278, 406

Packham, C., Young, S., Hough, J.H., Tadhunter, C.N., Axon., 1998, MNRAS, 297, 939

Serkowski, 1958, Acta.Astron., 8, 135

Sparks, W.B., Axon, D.J., 1999, PASP, in press

Stockton A., Ridgway S.E., Lilly, S., 1994, AJ, 108, 414

Stockton, A., Ridgway, S.E., 1996, in Cygnus A — Study of a Radio Galaxy, ed. C.L. Carilli & D.E., Harris (Cambridge: Cambridge University Press), 1
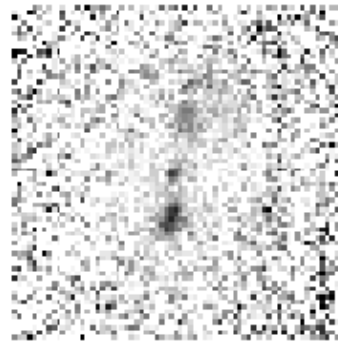
Tadhunter C.N., Scarrott S.M., Rolph C.D., 1990, MNRAS, 246, 163

Tadhunter C.N., Metz, S., Robinson, A., 1994, MNRAS, 268, 989

Tadhunter C.N., Packham, C., Axon, D.J., Jackson, N.J., Hough, J.H., Robinson, A., Young, S., Sparks, W., 1999, ApJ, 512, L91

Ueno S., Katsuji K., Minoru N., Yamauchi S., Ward M.J., 1994, ApJ, 431, L1

Ward M.J., Blanco P.R., Wilson A.S., Nishida M., 1991, ApJ, 382, 115

Ward M.J., 1996, in Cygnus A — Study of a Radio Galaxy, ed. C.L. Carilli & D.E., Harris (Cambridge: Cambridge University Press), 43

van der Marel, R., 1998: http://sol.stsci.edu∼marel/software.html

Figure 1. Infrared (2.0μm) polarization images of Cygnus A. Top left – total intensity (Stokes I) at full resolution; top right – polarization degree at full resolution; bottom left – polarized intensity at full resolution; and bottom right – polarization vectors plotted on a contour map of the polarized intensity image derived from the data smoothed with a 5×5 pixel box filter, with length of vectors proportional to the percentage polarization. The line segment in the intensity image shows the direction of the radio axis. At the redshift of Cygnus A, 1.0 arcsecond corresponds to 1.0 kpc for $H_0 = 75$ km s^{-1} Mpc^{-1} and $q_0 = 0.0$.
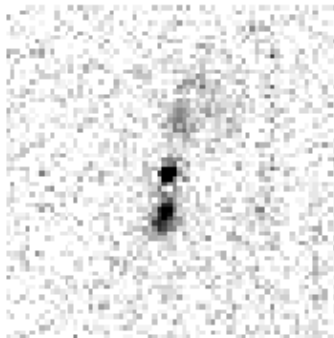
Intensity
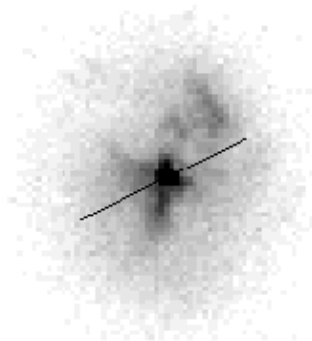
Polarization Degree

Polarized Intensity

E-Vector Directions

N

E

1 arcsec

20%